Proceedings of the 5th International Conference of Fluid Flow, Heat and Mass Transfer (FFHMT'18)
Niagara Falls, Canada – June 7 – 9, 2018
Paper No. 147
DOI: 10.11159/ffhmt18.147

Steady State Modelling, Experimental Validation and Performance Analysis of Thermo-Acoustic System

Salem Haggag, Ghaleb Ibrahim, Bader Al-Ajeel, Tasneem Suboh, Aly Tourk
School of Engineering, Mechanical Department, American University in Dubai
Dubai, United Arab Emirates
shaggag@aud.edu

Abstract **-** Thermo-acoustic refrigerators (TAR) pose several benefits over traditional refrigeration systems, mainly in eliminating the use of harmful refrigerants. In this paper, a thermo-acoustic refrigerator system is designed and experimentally tested. The applied operating parameters are the frequency of 501 Hz and one atmospheric mean pressure. The working medium is Helium-Air mixture. A dimensionless steady state mathematical model is used in the analysis as well as to establish the system main parameters. The system is designed and manufactured using a PVC material. The effect of the stack center position and frequency on the system coefficient of performance (COP) is experimentally and theoretically investigated. Two stacks are used in the design (Ceramic and Mylar) which are used to test the impact of the stack material on system performance. A loudspeaker and an amplifier are used to generate the acoustic power required for the system operation. For the Ceramic stack, a center position of 6.25 cm and a frequency of 501.541 yielded the most average temperature difference. The Mylar stack is tested at the same condition and yielded a better results compare to the Ceramic one. The experimental and the steady state model results show a good agreement which prove the validity of the system steady state model and its potential capabilities when comes to thermos-acoustics systems design and optimization.

Keywords**:** Thermo-Acoustic Systems, Steady State Modelling, Acoustic Waves.

1. Introduction

Thermo-acoustic refrigeration (TAR) is an eco-friendly refrigeration system that uses sound waves and a non-flammable mixture of inert gas (helium, argon, air) or a mixture of gases in a resonator to produce cooling. A TAR system uses the energy of sound or pressure waves to bring about refrigeration. It overcomes the drawbacks of conventional methods of the vapor compression system, air refrigeration system, etc., which require harmful refrigerants and moving parts such as compressor. Swift [1] discussed the fundamentals of thermos-acoustic engines and refrigerators, research in this field, and their commercial development. The TAR consists of four main components namely; the resonator, the stack, the acoustic driver and the heat exchangers as shown in Figure 1.

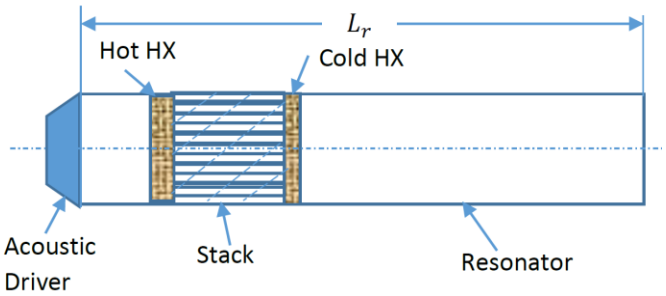

Fig. 1: Schematic of Thermos-Acoustic System.

The standing pressure wave generated by acoustic driver in the resonator causes back-and-forth motion of the gas from one end of the stack to the other thereby providing a mean of transporting energy. The gas near the pressure node gets cooled due to expansion and absorbs heat from the stack so one end of stack is cooled. This gas moves towards pressure antinode and gets heated due to compression giving off heat to the stack so the other end of the stack is heated. Thus, a

temperature gradient occurred along the stack length [2]. To obtain a standing wave a pressure wave generator such as loudspeaker driver is needed. Two parameters that are important to obtain a standing wave and obtain an effective temperature gradient across the stack are the frequency and decibels of the acoustic wave generated by the loudspeaker [3][4]. Usually the loudspeaker is controlled using a signal amplifier.

Understanding the Thermo-acoustic refrigeration (TAR) system operation is essential for its construction. Obtaining a suitable standing wave is crucial for efficient operation of the TAR system. On the other hand, the nodes and anti-nodes of the standing pressure wave are interchangeable with those of the standing displacement wave. The gas molecules undergo longitudinal oscillation when located at anti-nodes, and are stationary when situated at a node [2].

There are some research studies done on the performance of thermos-acoustic devices without stack [4-6]. They concluded that it is required to have different heat exchangers deign such as large ratio of exchanger area to sidewall area. In many thermos-acoustic devices, the stack is the core part. Extensive experiment and theoretical research done on the performance of thermos-acoustic devices with stack [2, 3, 4, 8-13]. When the stack is positioned between two pressure anti-nodes, the gas particles will go through compression (high pressure anti-node) followed by expansion (low pressure anti-node). During the compression, the temperature increases as per the Ideal Gas Law and the wall of the plates then absorbs the resulting heat. The expansion results in decreasing temperature and so the gas particles are now colder than the stack plates, the particles will absorb the heat from the walls of the plates. This process occurs repeatedly, which form the basis of thermos-acoustic refrigerator systems cooling mechanism.

The resonator tube is the component in which the medium transfers the pressure change back and forth within the tube. The length, weight, and shape of the tube are all designed to keep losses such as viscous and leaking at a minimum. The length of the resonator tube dependents on the resonance frequency. The tube must also be designed leakage free, which can be harmful to the operation of the TAR system [2]. The terminating end of the resonator tube is either a closed end or it can have a volume buffer (cone or spherical shaped cavity) to simulate an open end. When a sound wave with a positive phase hits the open end, it will stay positive when it travels back and vice versa. This amplify the effect of two or more waves interacting with each other in a standing wave when having the same phases [13]. Developments and advancements aimed to improve the efficiencies of TAR systems are still undergoing. Lycklama a Nijeholt et al [14] and Yu Z. et al [15] investigated the use of travelling waves or combined standing and traveling waves to improve the thermos-acoustic engines. Lycklama a Nijeholt et al [14] obtained results that showed an increase of the dynamic pressure. Yu Z. et al [15] have concluded that such concept could be very attractive.

2. Design and Construction of the Proposed Thermos-Acoustic Refrigerator (TAR) System

2.1. TAR System Components

Figure 2 shows the main components of the proposed TAR system. The system consists of a loudspeaker hosted in a speaker housing, a resonator tube, buffer volume and a stack. A function generator is used to control a sound amplifier that in turn is connected to the loudspeaker. Two temperature sensors are used to measure the temperature gradient around the stack element. One sensor is used for the cooled side of the stack and the other is used for the hot side of the stack. Their temperature range is −40.0℃~99.9℃ with an accuracy of 0.1℃ [16]. Figure 3 shows the manufactured prototype of the TAR system. It is important to note here that both the function generator and the sound amplifier are not shown in Figure 2 and Figure 3.

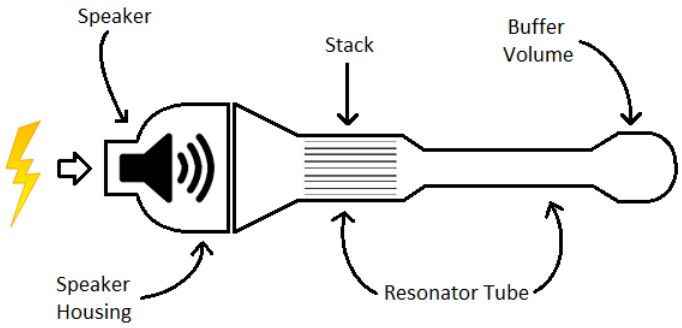

Fig. 2: Schematic Diagram of the Proposed TAR System.

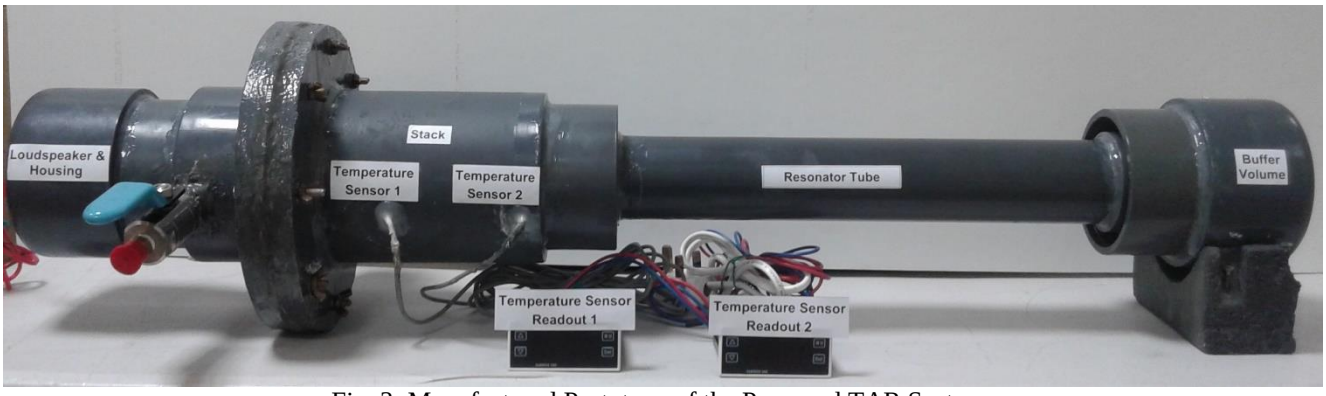

Fig. 3: Manufactured Prototype of the Proposed TAR System.

2.2. TAR System Design Parameters

The structure and performance of the TAR system depend on three main factors: the internal operating pressure, the operating frequency of the loudspeaker, and the working gas that is injected into the resonator tube.

a) Operating Pressure:

A sound wave's energy density is directly proportional to the pressure of the medium in which the sound wave is propagating. Therefore, increasing the pressure inside the resonator tube is beneficial and full advantage of the sound energy produced by the loudspeaker driver is utilized. The attainable cold temperature and the cooling power crucially depend on the dynamic pressure and operation near the resonant frequency of the system [17]. Initially, an operating pressure of 10 bar is chosen for the prototype. However, such high pressure requires a high pressure vessel and high pressure seals especially when using Helium, which has a small molecular size - almost 7 times smaller than air molecule. For leakage free operation, the average operating pressure is instead chosen to be atmospheric pressure.

b) Working Gas

A high sound velocity, thermal conductivity, and inertness of the medium in which the sound wave is traveling are desirable effects for the operation of the TAR system, and Helium possesses all of these characteristics [2]. The speed of sound in Helium is about three times the speed of sound of air and its thermal conductivity is seven times the thermal conductivity of air [3]. Since the spacing of the stack is proportional to the square of the thermal conductivity, a high thermal conductivity of the gas is fevered [2]. As such, Helium would have been a good choice. In the proposed TAR system, Helium was injected into the resonator tube and mixed with existing air, and so the operating gas is considered as a Helium-Air mixture.

c) Operating Frequency

The energy density of a sound wave is also a linear function of the acoustic resonance frequency. Thus, a high resonance frequency is desirable. However, the acoustic frequency is inversely proportional to the square of the thermal penetration depth or, in other words, the spacing between the stack's plates [2]. This means that a higher resonance frequency would result in a very small stack spacing, which would be extremely difficult to manufacture. Furthermore, a higher acoustic frequency would also produce a higher pitched sound, which would become harmful for human hearing.

d) Stack Design

The stack is often called the heart of the TAR system, because it is what enables the sound waves to produce a cooling effect. The main factors which affect the generation of a temperature gradient across the stack, are: the stack material and the spacing between the stack's plates. The stack material requires to have low thermal conductivity. This is to maintain high temperature gradient along the stack. In the proposed TAR system, both Mylar and Zirconia Ceramic stacks are used. Mylar stack has a good retention of its physical properties over a wide range of temperatures. Both Ceramic and Mylar stacks possess a low thermal conductivity as shown in Table 1.

Table 1: Thermal properties of stack materials.

	Zirconia ceramic	Mylar
Thermal Conductivity (K)	$2\ \frac{W}{m \cdot k}$	$0.15\ \frac{W}{m \cdot k}$
Heat Capacity ($\boldsymbol{c_p}$)	$418\ \frac{J}{kg \cdot k}$	$1172.3\ \frac{J}{kg \cdot k}$

The stack is not a standard component but is manufactured from Ceramic and Mylar. Fig. 4 shows the stacks used in the TAR system. A cylindrical block with a rectangular cavity is designed and manufactured to hold the stack inside the resonator. The stack holder is chosen to be rigid with a low thermal conductivity, since it must not conduct the heat produced by the hot end of the stack.

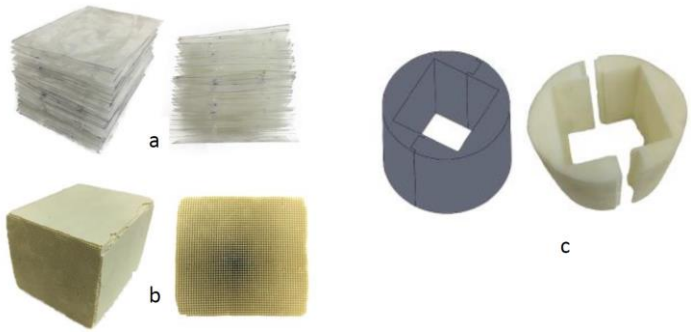

Fig. 4: Stacks Used in the TAR System, a) Mylar, b) Ceramic stack, c) Stack holder.

The stack spacing controls the interaction between the gas particles and the walls of the stack. Large spacing will reduce heat exchange between the gas particles and the walls. If the spacing is too small, viscous effects between the walls and the gas may obstruct the motion of the gas particles [20]. The thermal penetration depth, δ_k, becomes an important criterion for the stack spacing. Tijani et al [18] studied the influence of the plate spacing in the stack on the behavior of the refrigerator. They showed that the parallel plate geometry is the best, and that a sheet spacing in the stack of about $3\delta_k$ should be optimal for the cooling power.

e) Resonator Tube Design

The design of the resonator tube is of two folds; 1) the selection of material (which depends on operating pressure), the acoustic reflectivity and working gas and (2) dimensioning which is depending on the frequency. Polyvinyl chloride (PVC) material has a low thermal conductivity and is able to sustain pressures up to 12 bar, so rigidity and durability are not a problem [19]. Dimensioning the resonator tube has been primarily orientated around the operational frequency and obtaining a standing wave. A standing wave in the resonator tube can be either half-wavelength (L = λ/2) or quarter-wavelength (L = λ/4). The length of the resonator tube can be calculated for quarter and half-wavelength using the following Equations [20].

$$L_r = \frac{\sqrt{\gamma RT}}{4f} \tag{1}$$

$$L_r = \frac{\sqrt{\gamma RT}}{2f} \tag{2}$$

Where L_r is the length of the resonator, γ is the specific heat ratio, R is the gas constant, f is the wave frequency and T is the operating temperature. The resonator tube length is calculated for a frequency range 100 Hz to 600 Hz. A shorter resonator has the advantage of less cost, and less power loss. Tijani [2] showed that the total dissipated energy is proportional to the surface area of the resonator, a λ/4 resonator will dissipate only half the energy dissipated by a λ/2

resonator. Hence, a λ/4 resonator is preferable for the proposed TAR system in this work. Hofler [21] and Tijani [2] showed that the λ/4-resonator could be further optimized by reducing the diameter of the resonator part on the right of the stack. To meet this requirement, the large diameter and small diameter PVC tubes are selected as 4.3 in and 2.4 in, respectively. Tijani [2] recommends that the large diameter tube should consist of only 25% of the total resonator tube length. As a result, the length for the large diameter tube was chosen as 135 mm while the length of the small diameter tube was chosen as 365 mm. At the end of the resonator, tube is the buffer volume.

3. Experimental Work Procedure and Results

To conduct appropriate experiments on the TAR prototype, three variables are changed to see their effects on system performance; the Stack center position, the frequency, and the stack material. The stack center positions tested, measured from the start of resonator, were 6.25 cm, 10.75 cm, and 12.25 cm. Six operating frequencies are tested, from 101.541 Hz to 601.541 Hz with an increment of 100 Hz. The tests are run for two types of stacks; a ceramic stack, and a Mylar sheet stack.

The first three tests involved positioning the center of the ceramic stack at the three positions of 6.25 cm, 10.75 cm, and 12.25 cm. At each stack center position, the running time for all six frequencies is 900 seconds (or 15 minutes) each. The position and frequency at which the stack performed best is then chosen, and the Mylar stack is tested at that position and frequency for 15 minutes too. Six Frequencies at Stack Center Position of 6.25 cm results are shown in Figure 5. The temperature gradient that occurred after each test are listed in Table 4. As can be seen, the theoretical frequency of 501.541 Hz did indeed yield the highest temperature difference and perform best. The same previous test is repeated for a stack center position of 10.75 cm as can be seen in Figure 6. Similarly, Figure 7 shows the experimental results for a stack center position of 12.25 cm.

The temperature differences at each frequency are listed in Table 4. As it can be seen that for a stack center position of 6.25 cm, a maximum temperature gradient is achieved at a frequency of 501.541 Hz. In addition, the maximum temperature gradients for 10.75 and 12.25 are achieved at 101.541 and 301.541 respectively. From the results, it is obvious that there is neither a clear relation between the frequency and the stack center position nor a clear relation between frequency and temperature difference. Two Frequencies (501.541 and 601.541) for the Mylar stack are tested at a position of 6.25 cm. The test results are shown in Figure 8. The ceramic stack is replaced with the Mylar stack, whose center was positioned at 6.25 cm from the resonator tube since that position yielded the highest temperature average in the ceramic stack tests. The frequencies of the Mylar stack test are chosen because they are the two best performing frequencies at a position of 6.25 cm in the ceramic stack test.

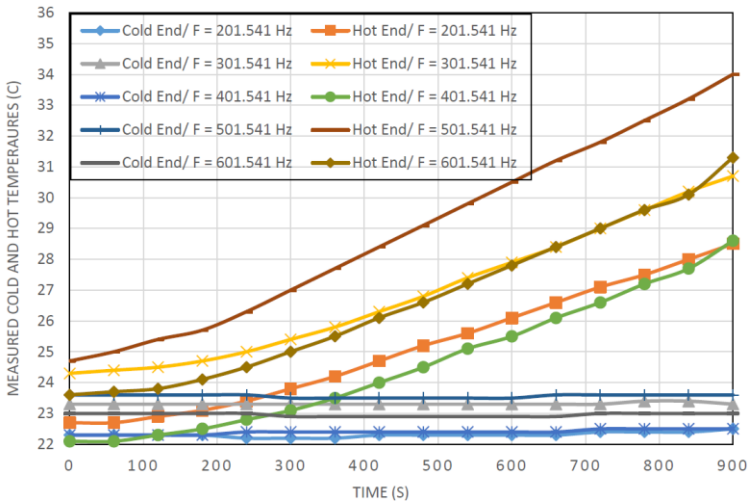

Fig. 5: Cold and hot Temperatures at stack center position 0.0625m for ceramic stack.

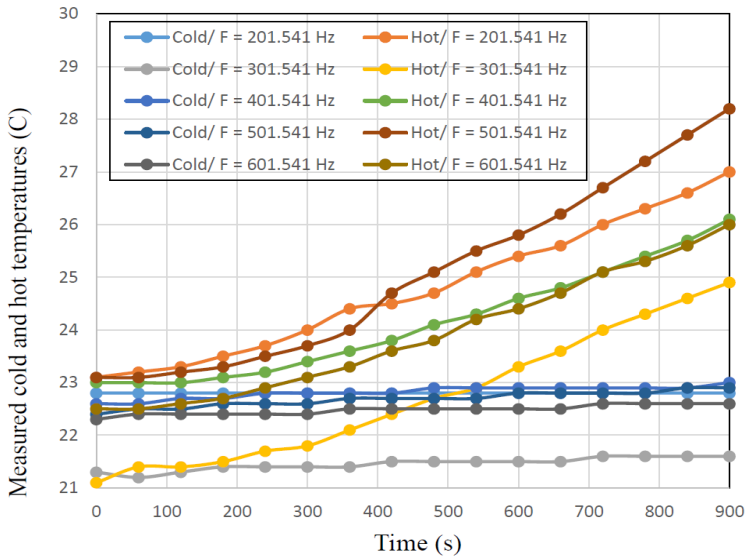

Fig. 6: Cold and hot Temperatures at stack center position 0.1075 m for ceramic stack.

The temperature difference at both frequencies can be seen in Table 5. Both results yield a higher temperature difference than that produced by the ceramic stack operating at the same parameters. For this reason, the Mylar stack is chosen as the stack on which the final experiment will be performed. The parameters of the final experiment are all based on the parameters that yielded the best results in the earlier experiments. The stack was placed at a stack center position of 6.25 cm, the operating frequency was inputted as 501.541 Hz, the stack material chosen was Mylar. The final experiment is run for one hour, and the temperature of both ends of the stack were recorded minute-by-minute. The experimental results of the temperature at each end of the stack versus time can be seen in Figure 9. As it can be seen, the temperature difference between the cold and hot ends of the stack at the end of the experiment was 26.4 degrees.

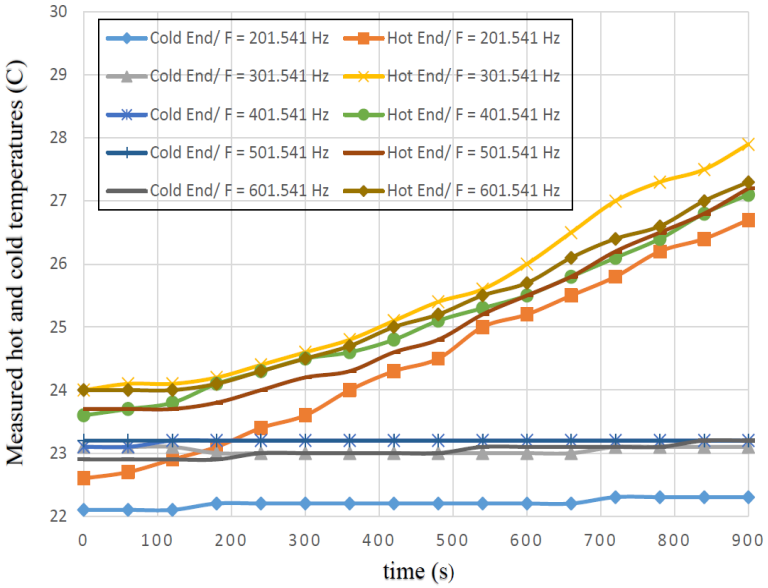

Fig. 7: Cold and hot Temperatures at stack center position 0.1225 m for ceramic stack.

Table 4: temperature gradient at three different stack center positions/ Ceramic Stack.

	Temperature Difference (K) at stack centered position		
Frequ	**6.25**	**10.7**	**12.2**
101.5	0.3	5.9	1
201.5	6	4.2	4.4
301.5	7.4	3.3	4.8
401.5	6.1	3.1	3.9
501.5	10.4	5.3	4
601.5	8.3	3.4	4.1
Avera	6.4	4.2	3.7

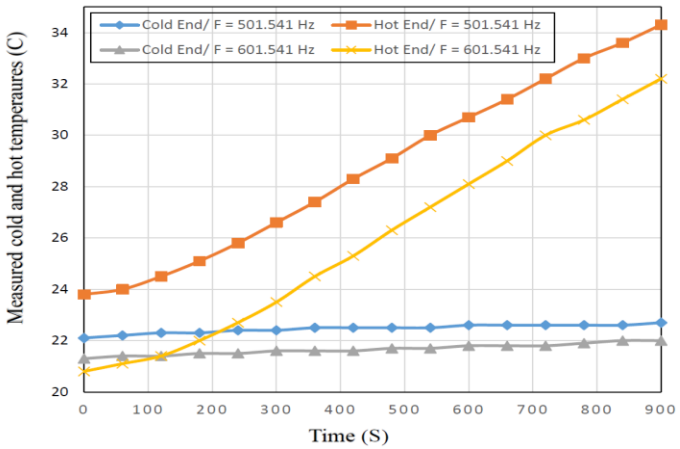

Fig. 8: Cold and hot Temperatures at stack center position 0.06255 m for Mylar stack.

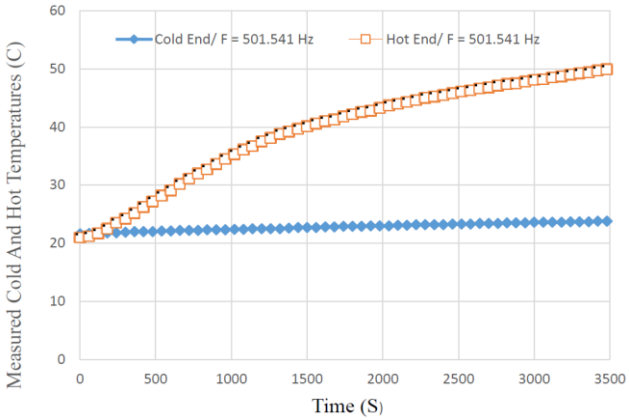

Fig. 9: Cold and hot Temperatures at stack center position 0.06255 m for Mylar stack.

Table 5: Temperature difference for various frequencies at three different stack center positions/ Mylar stack.

Frequency (Hz)	Temperature Difference (K) at stack center position of 6.25 cm
501.541	11.6
601.541	10.2

4. Discussion of Experimental Results

From the experimental results two observation can be obtained; (1) the Mylar stack performed better than the ceramic stack, yielding higher temperature differences at the same frequencies and during the same time. This can be attributed to Mylar's more superior thermal properties compared to ceramic, as can be seen in Table 1. Its lower thermal conductivity means less heat conduction across the stack. Also, higher specific heat capacity means storing more energy to maintain its temperature, so that the cold side of the stack can remain at a low temperature. (2) the most obvious observation is that the temperature at the cold side of the stack is not decreasing. Several factors can attribute to this, mainly three; the effects of thermal conductivity across the stack, the presence of air in the medium, and effects of pressure on gas particles.

Effects of thermal Conductivity across the stack: Conductive effects occur naturally when a temperature gradient is present. Even though the heat transfer between the hot and cold side is inevitable. Both materials of the two stacks possess low thermal conductivities, but the effects of conductivity were still present. This can be seen from the slight increase of the cold temperature for the Mylar stack at 501.541 Hz by 0.6 K.

Effects of Pressure on Gas Particles: The effect of operating pressure in a TAR system is significantly important, especially in terms of decreasing the temperature on the cold end of the stack. This TAR prototype is designed to work at atmospheric pressure. Other researchers obtained a similar results when the run the system at atmospheric pressure. Ryan T. S. [19] ran his system at atmospheric pressure and obtained an increase in hot temperature with very slight decrease in the cold temperature. Barot and Coit [22] ran their system with a mixture of helium and air at 1 and 2.5 atmospheric pressures. A temperature gradient of 1.5 at 1 atmospheric pressure and a temperature gradient of 66 K at 2.5 atmospheric pressure are obtained. The obvious reason for this phenomenon is because of gas behaviour's dependency on pressure. At atmospheric pressure, the gas particles are typically scattered far apart, as opposed to when they are pressurized and forced to interact with each other more frequently. Heat dissipation and heat absorbance occur more effectively when the gas particles are compacted and forced to interact.

Presence of Air in the Medium: Air has a thermal conductivity lower than that of helium, and it acts like an insulator. The effects of having air in the medium can be compared to having a "damping" effect in the system, limiting the system's performance.

5. Steady State System Model

The temperature difference $\Delta T = T_H - T_C$ between the both ends of the stack plate can be obtained using the linear theory as suggested by Marx and Blanc-Benon [9] as follows;

$$\Delta T = -\frac{\alpha_1 L y_o P_A^2 \sin(2\kappa \cdot xs)\, A_1}{4\,\rho_m c[\alpha_2 y_o K + l\, K_s - \frac{y_o C_p}{4\,\omega\rho_m\, C^2(1-P_r)} P_A^2(1-\cos(2\kappa \cdot xs))\, A_2]} \tag{3}$$

where A_1, A_2 are defined in equations 4 and 5, c is speed of sound, C_p , C_s are the fluid and stacks specific heat respectively, K, K_s are the fluid and stacks thermal conductivity respectively, L is the length of the stacks, P_A is the maximum amplitude of the pressure oscillation, P_r = is the Prandtl number, κ is wave number, x_s is the centre stacks position, ρ_m mean time average density, y_o = is half the spacing between two stacks plates.

$$\text{Where } A_1 = \frac{\delta_k}{2y_o} \frac{1-\frac{\delta_v}{2y_o}+\sqrt{P_r}}{(1+\varepsilon_o)(1+P_r)\left(1-\frac{\delta_v}{y_o}+\frac{1}{2}\left(\frac{\delta_v}{y_o}\right)^2\right)} \tag{4}$$

where δ_v, δ_k are the viscous, thermal penetrations depth as defined in equations 7 and the subscripts f and s stand for fluid and stacks respectively and ε_o is defined in equation 6.

$$A_2 = -\frac{\delta_k}{2y_o} \frac{(1-P_r)(1-\sqrt{P_r}+P_r+P_r\varepsilon_o}{(1+\varepsilon_o)\left(1+\sqrt{P_r}\right)(1+P_r)\left(1-\frac{\delta_v}{y_o}+\frac{1}{2}\left(\frac{\delta_v}{y_o}\right)^2\right)} \tag{5}$$

$$\varepsilon_o = \frac{\left(\rho_m C_p \delta_k\right)_f}{\rho_s C_{p_s} \delta_{k,s}} \tag{6}$$

$$\delta_k = \sqrt{\frac{2K}{\rho_m c_p \omega}} \quad ; \quad \delta_{k,s} = \sqrt{\frac{2K_s}{\rho_m c_p \omega}} \quad ; \; \delta_v = \sqrt{\frac{2\upsilon}{\omega}} \; ; \; \omega = 2\pi f \tag{7}$$

where υ is kinematic viscosity, $\omega$is angular frequency and f is the frequency.

The coefficients $\alpha_1 and\ \alpha_2$ are to account for the nonlinearity behavior at both end of the stack plates. They are depending on various parameters such as thermal conductivities, stack position, stack spacing, stack length and Mach number. For the range of Mach number and the stack length applied in this current work, they are approximately 0.9 and 1.2 respectively [9]. The steady state system equations 3-7 are solved to obtain the temperature difference for a frequency range from 100 – 600 Hz at drive ratio, DR, range from 1% - 3%. The results are compared with the experimental results as shown in figure 10. The experimental results are obtained after 900 seconds and steady state is still far from being reached, Figure 9 shows that after 3500 seconds the temperature difference reached 26.4. Therefore it can be easily conclude that the linear model solved under the same experimental conditions underestimate the temperature gradient along the stack. Marx and Blanc-Benon [9] referred this discrepancy to the complex dependency of $\alpha_1 and\ \alpha_2$. In addition the other possible explanation for the large deviation is due to stack length so the stack length used is too long.

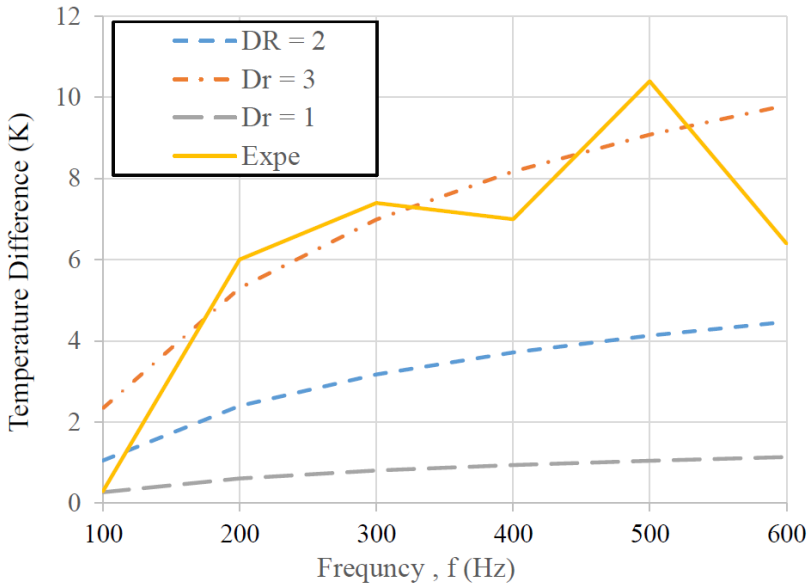

Fig. 10: Temperatures difference at stack centre position 0.06255 m for ceramic stack.

6. Conclusion

In this paper the design and manufacturing of a thermoacoustic refrigerator is discussed. The construction of the different parts of the refrigerator is described in detail. The system has been assembled and the experimental measurements were taken at three stack centered positions namely 0.0625 m, 0.1075 m and 0.1225 m for frequency range of 200 Hz – 600 Hz. The measured data gave an indication of performance as expected. A maximum temperature gradients of 26.4 is produced with 0.0625 stack centered position/ Mylar stack with a frequency of 501 Hz. Due to the low operation pressure, the cold temperature remained almost unchanged. The obtained temperature gradient for Mylar stack, due to thermal properties, was higher than that for ceramic stack. The linear model used to determine the temperature difference underestimate the experimental results. On the other hand the COP, Qc and W agrees well literature. The COP has maximum at 325 Hz. Where the maximum temperature difference occurs at around 500 Hz.

References

[1] G. W. Swift, "Thermoacoustic engines and refrigerators," *Physics Today*, vol. 48, pp. 22-28, 1995.

[2] M. E. H. Tijani, "Loudspeaker-Driven Thermoacoustic Refrigeration," Ph.D. Dissertation, Technische Universiteit Eindhoven, 2001,

[3] B. Al Ajeel, T. Suboh and A. Tourk, *Thermoacoustic Refrigerator, Design Project Report*. AUD, 2016.

[4] M. E. H. Tijani, J. C. H. Zeegers, A. T. M. M. De Waeel, "Design of themoacosutic refrigerator," *Cryogenics*, vol. 42, pp. 49-57, 2002.

[5] B. Asgharian, and K. I. Mateveev, "Numerical Modelling of thermoacoustic No-Stack," *Engineering Application of Computional Fluid Dynamics*, vol. 6, no. 3, pp. 346-355, 2012.

[6] S. R. Wakeland and R. M. Keolian, "Thermoacoustics with idealized heat exchangers and no stack," *J Acoust Soc Am.*, vol. 111, no. 6, pp. 2654-2664, 2002.

[7] S. R. Wakeland, R. M. Keolian, "Calculated effects of pressure driven temperature oscillations on heat exchangers in thermosacoustic devices with and without stack," *J Acoust Soc Am.*, vol. 116, no. 6, pp. 294-302, 2002.

[8] L. Zoontjens, C. Q. Howard, C. A. Zander, B. S. Cazzolato, "Development of a low cost loudspeaker-Drven thermoaccoustic Refrigerator," *Proceedings of Acoutics*, pp. 1-7, 2005.

[9] D. Markx, Ph. Balnc-Benon, "Numerical Calculation of the temperature difference between the extremities of a thermosacoustic stack plate," *Cryogenics*, vol. 45, pp. 163-172, 2005.

[10] S. L. Garrett, J. A. Adeff, T. J. Hofler, "Thermoacoustic Refrigertor for Space Applications," *J Thermophysics and Heat Transfer*, vol. 7, no. 4, pp. 595-599, 1993.

[11] M. E. H. Tijani, J. C. H. Zeegers, A. T. M. M. De Waeel, "Construction and Performance of Thermoacoustic Refrigerator," *Cryogenics*, vol. 42, pp. 59-66, 2002.

[12] J. Newman, B. Cariste, A. Queiruga, I. Davis, B. Plotnick, M. Gordon, "Thermoacoustic Refrigeration," *GSET Research Journal*, pp. 1-9, 2006.

[13] Y. A. Abakr, M. Al Atabi, and C. Baiman, "The influence of wave patterns and frequency on thermo-acoustic cooling effect," *Journal of Engineering Science and Technology* (*JESTEC*), vol. 6, no. 3, pp. 392-396, 2011.

[14] J. A. Lycklama à Nijeholt, M. E. H. Tijani, S. Spoelstra. Simulation of a traveling-wave thermoacoustic engine using computational fluid dynamics. *Journal Acoustical Society of America* 2005, **118**:4, 2265.

[15] Z. Yu, A. J. Jaworski, S. Scott Backhaus, "Travelling-wave thermoacoustic electricity generator using an ultra-compliant alternator for utilization of low-grade thermal energy," *Applied Energy*, vol. 99, no. 11, pp. 135-145, 2012.

[16] *Temperature Controller SU-103SR/SU-105DA-N Manual*. [Online]. Available: http://fse-automation.com/content/samwon/samwon-datasheet/SU-105DA-N--SU-103SR.pdf

[17] R. C. Dhuley, M. D. Atrey, "Investigations on a Standing Wave Thermoacoustic Refrigerator," *Cryocoolers*, vol. 6, no. 335, 2011.

[18] M. E. H. Tijani, J. C. H. Zeegers, and A. T. A. M. De Waele, "The optimal stack spacing for thermoacoustic refrigeration," *The Journal of the Acoustical Society of America*, vol. 112, no. 1, p. 128133, 2002.

[19] T. S. Ryan, **"**Design and control of a standing wave thermosacoustic refrigerator," M.S. Thesis, University of Pittsburgh, 2009.

[20] N. Mohd-Ghazali, M. Anwar, H. M. A. Nurudin, N. H. M. A. Settar, "Thermoacoustic Cooling With No Refrigerant," *International Journal of Technology*, vol. 3, pp. 234-241, 2011.

[21] T. J. Hofler, "Thermoacoustic Refrigerator Design and Performance," Ph.D. Dissertation, University of California San Diego, 1986.

[22] V. Barot and D. Coit, *Experiments with a Thermoacoustic Refrigerator*. Worcester Polytechnic Institute, A Major Qualifying Project Report, pp. 57-58, 2009.

[23] A. A. Omar M, M. Al Zubi, "Demonstrating of a Standing Wave -Thermoacoustic Refrigerator," *Int. J. of Thermal & Environmental Engineering*, vol. 6, no. 2, pp. 75-81, 2013.

[24] K. Assawamartbunlue, C. Wantha, "Experimental Investigation on the Optimal Operating Frequency of a Thermoacoustic Refrigerator," *Int J Mechanical, Aerospace, Industrial, Mechatronic and Manufacturing Engineering*, vol. 9, no. 5, pp. 779-782, 2015.